Diffusion and Consumption of Oxygen in the Superfused Retina of the Drone (*Apis mellifera*) in darkness

M. TSACOPOULOS, S. POITRY, and A. BORSELLINO

From the Experimental Ophthalmology Laboratory and the Department of Physiology, School of Medicine, University of Geneva, Geneva, Switzerland. A. Borsellino's present address is the Laboratorio di Cibernetica e Biofisica, C.N.R., Camogli, Italy.

ABSTRACT Double-barreled O_2 microelectrodes were used to study O_2 diffusion and consumption in the superfused drone (*Apis mellifera*) retina in darkness at 22°C. P_{O_2} was measured at different sites in the bath and retina. It was found that diffusion was essentially in one dimension and that the rate of O_2 consumption (Q) was practically constant (on the macroscale) down to P_{O_2}s < 20 mm Hg, a situation that greatly simplified the analysis. The value obtained for Q was 18 ± 0.7 (SEM) μl O_2/cm^3 tissue · min (n = 10), and Krogh's permeation coefficient (αD) was 3.24 ± 0.18 (SEM) × 10^{-5} ml O_2/min · atm · cm (n = 10). Calculations indicate that only a small fraction of this Q in darkness is necessary for the energy requirements of the sodium pump. The diffusion coefficient (D) in the retina was measured by abruptly cutting off diffusion from the bath and analyzing the time-course of the fall in P_{O_2} at the surface of the tissue. The mean value of D was 1.03 ± 0.08 (SEM) × 10^{-5} cm^2/s (n = 10). From αD and D, the solubility coefficient α was calculated to be 54 ± 4.0 (SEM) μl O_2 STP/cm^3 · atm (n = 10), ~1.8 times that for water.

INTRODUCTION

The drone (*Apis mellifera*) retina has features that make it a tissue in which it is particularly interesting to measure the degradation of the stores of metabolic substrate, the production of ATP, and the utilization of energy in pumping ions or synthesizing biochemical molecules. The retina is comprised of only two, essentially uniform, cell populations: the photoreceptors, which respond directly to light stimulation (Baumann, 1968 and 1974), and the glial cells. The former contain mitochondria and no histologically detectable glycogen, whereas the latter contain much glycogen and few, if any, mitochondria (Perrelet, 1970). This arrangement indicates a compartmentation of metabolism. There is experimental evidence that in the isolated head preparation used in electrophysiological experiments (and also in the present work), the glycogen in the glia is the main store of metabolic substrate, and it has been shown that, when the photoreceptors are stimulated by light, the glycogen turnover in the glia increases (Evêquoz et al., 1978). Part of the energy is used

to sustain transmembrane ion fluxes, and fluxes of one of the major ions, potassium, have been measured with ion-selective microelectrodes (Coles and Tsacopoulos, 1979). The present paper is intended as a first step toward relating the energy produced or used by these processes to the O_2 consumption in the photoreceptors.

In addition, a more specific question might be answered by an analysis of retinal O_2 consumption: it has been suggested that phototransduction (the generation of a receptor potential after absorption of light by the photopigment molecules) might require ATP beyond that necessary for the maintenance of transmembrane ionic concentration gradients. The evidence comes primarily from experiments in which the effect of blocking oxidative metabolism on the receptor potential was studied. Such experiments have been performed not only on the drone (Baumann and Mauro, 1973) but also on *Drosophila* (Wong et al., 1976), the ventral and lateral eyes of *Limulus*, and the lateral ocelli of *Balanus* (Borsellino and Fuortes, 1968; Lantz and Mauro, 1978).

In the superfused drone retina preparation (Baumann, 1968), stimulation with a single flash of light causes a fall in P_{O_2} in the tissue, within 1 s, that can be as great as 40 mm Hg (Tsacopoulos and Lehmenkühler, 1977). However, a quantitative analysis of such a change can be made only if the rate of O_2 consumption (Q) in the dark and also the coefficients of diffusion (D) and solubility (α) of O_2 in the tissue are known. The present paper provides this basic information. O_2 consumption in a worker bee retina has already been measured (with a micro-Warburg technique) by Autrum and Tscharntke (1962) and Hamdorf and Kaschef (1964), but it seemed necessary to remeasure it in the drone under our experimental conditions. In our work in progress on the kinetics of change in Q, the rapid response of the O_2 microelectrode makes it the tool of choice, and we have chosen to use it also for the steady-state measurements. The macroscopically uniform nature of the drone retinal tissue and the simple pattern of diffusion that we impose on it make it possible to calculate Q and αD from the P_{O_2} profile within the tissue and the bathing medium. D was measured by following the decay of the P_{O_2} at the surface of the retina when the O_2 supply was abruptly suppressed. The value that we find for α is considerably greater than that generally assumed for biological tissues.

METHODS

Measurement of Q and αD

With P_{O_2}-sensitive microelectrodes, steady-state P_{O_2} was measured at intervals along a line perpendicular to the tissue surface, in the medium above the tissue and within the tissue itself. Q and αD were derived from these P_{O_2} profiles as described by Ganfield et al. (1970) (cf. Theory section for details). Q was calculated from the flux of O_2 at the tissue surface and the depth of tissue oxygenation. For the measurement of αD, a major requirement of this technique is the validity within the tissue, on the macroscale, of the one-dimensional diffusion equation for the P_{O_2}. If this condition is met, $Q/\alpha D$ can be calculated from the P_{O_2} profile. The analysis made by Connelly et

al. (1953) and Mahler (1978 *a* and 1978 *b*) is not directly applicable to our experimental situation. In their study moist gas was used to oxygenate the nerves and muscles, but in our study the O_2 was dissolved in flowing Ringer's solution, and consequently the P_{O_2} at the surface of the tissue could be varied. Ringer's solution, instead of gas, was used so that it would be possible to study the effect of changing the ionic environment on the Q of the photoreceptors.

O_2 Microelectrode

The technique of making double-barreled O_2-sensitive microelectrodes has been described (Tsacopoulos and Lehmenkühler, 1977). The technique was slightly modified to make Pt double-barreled microelectrodes with recessed tips, which, in principle, allow quantitative measurements of local P_{O_2} in tissue, since the O_2 diffusion field is restricted to the recess (Schneiderman, 1975; Fatt, 1976). For recess-type microelectrodes, the etched Pt (tip diameter <1 μm) is passed through melted Elephant brand shellac (Thew Arnott, Wallington, Surrey, England) so that a ball of shellac forms over the tip. Thus protected, the Pt is pushed down one barrel of a micropipette (borosilicate "theta" tubing) until it is stopped by the constriction of the taper of the micropipette. Then, while viewed through a microscope, the shellac is heated and melted (Tsacopoulos and Lehmenkühler, 1977). By trial and error, a temperature is found at which the shellac melts, but remains viscous, so that it does not run toward the tip but retreats a little, leaving free the extreme tip of the Pt. Then, under continuous heating, the Pt is pushed through the melted shellac. While the Pt moves towards the tip, the melted shellac flows slowly with the Pt. When the Pt is at the desired distance from the tip (30–40 μm), heating is stopped and the shellac hardens around the Pt leaving only the extreme tip uncovered (Fig. 1: *inset*). The other barrel of the micropipette is filled with Ringer's solution and used as a reference electrode. These microelectrodes were found to have the O_2 currents predicted by theory (Schneiderman and Goldstick, 1976) for a recess of 30 μm and a tip diameter of 1 μm (0.032 pA/mm Hg of P_{O_2}).

The electronic setup for measurement of P_{O_2} with double-barreled microelectrodes has been described in detail (Lehmenkühler et al., 1976; Tsacopoulos and Lehmenkühler, 1977). The voltage between the Pt tip and the immediate surroundings measured by the reference barrel is clamped to a constant value. With this technique, the existence and stability of a well-defined "polarization plateau" is not critical because voltage perturbations often occurring in excitable tissues are compensated in ~20 ms (Lehmenkühler et al., 1976). The polarization voltage was always −580 mV.

Performance of the O_2 Microelectrodes

STABILITY The isolation of the Pt with shellac and borosilicate glass appeared good, since the O_2 current remained stable for many days or even months (Fig. 1) (see also Tsacopoulos and Lehmenkühler [1977]). During the experiments the O_2 current measured in air-equilibrated solutions reached a stable value in about 20 min after the polarization voltage was turned on (see also Whalen et al. [1967]). However, when the microelectrode was used in intratissue P_{O_2} measurements, after the first tissue penetration, there was a 2–8% ($n = 50$ microelectrodes) decrease of the slope of its initial calibration curve when it was rapidly withdrawn to the bath. This phenomenon was probably not related to the Pt itself, because it has been observed also with gold "Whalen-type" microelectrodes (Whalen et al., 1967) made in this laboratory. If the electrode was kept in the bath after the tissue penetration, the lost O_2 current recovered in about 10 min. It was also observed that: (*a*) the lower the O_2 current of

the electrode, the less the drop of the slope after tissue penetration (relatively fine microelectrodes were used [0.035–0.10 pA/mm Hg of P_{O_2}]) and (*b*) penetrations in the superficial layers of the tissue (relatively high P_{O_2}) did not cause any substantial O_2 current drop. To explore more factors that could affect the stability of O_2 microelectrodes used repetitively in intratissue measurements, we made special recess-type microelectrodes with a polystyrene membrane. The membrane was applied to a column of 50% glycerine and 5% gelatine in tris(hydroxymethyl)aminomethane

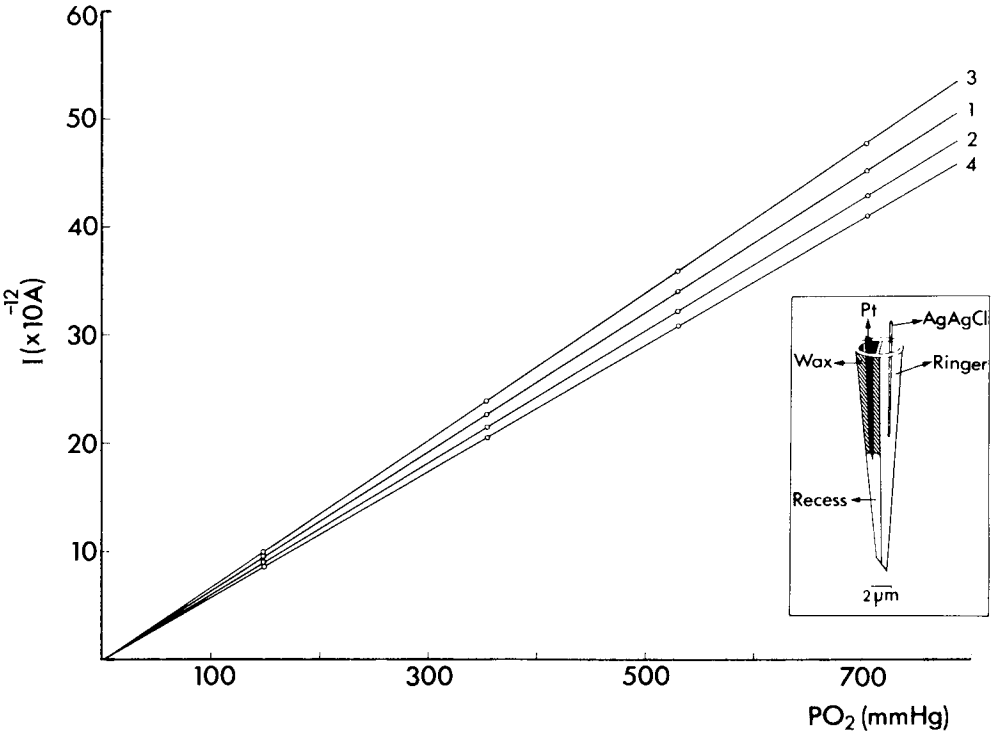

FIGURE 1. Calibration curves of a microelectrode. There is a linear relationship between P_{O_2} (abscissa) and current (ordinate). Curve 1 was obtained on the day of fabrication of the electrode. Then, the electrode was repeatedly used in experiments and calibrated several times before and after tissue penetration. Curves 2–4 are samples obtained 1 wk, 1 mo, and 3 mo later than curve 1, respectively. The *inset* is a schematic representation of a typical double-barreled recess-type microelectrode. In some experiments the recess was filled with a membrane (see also text).

(Tris)-buffered Ringer's solution that filled the recess. The polystyrene membrane and the material trapped inside the recess reduced the O_2 current by only ~20%, but it prevented a hypothetical contamination of the Pt by macromolecules. The results obtained with these microelectrodes in some experiments were identical to those obtained with uncovered recess Pt or Au (Whalen-type) microelectrodes. However, since the technique for the membrane application is laborious, the bulk of the experiments were performed with uncovered recess-type Pt microelectrodes.

CALIBRATION These electrodes were calibrated repeatedly during an experiment and showed excellent linearity in Ringer's solution at 22°C over the P_{O_2} range of 0–700 mm Hg (Fig. 1). An easy way to obtain the current at zero P_{O_2} (the so-called "dark current"; Davies, 1962) was to place the electrode at the beginning and at the end of the experiment deep inside the tissue and then superfuse the retina with N_2-equilibrated solution under light stimulation (see Results). A similar method has been used in other tissues (Takahashi et al., 1966; Mahler, 1978 *a*). The value obtained with this technique was compared with that obtained by dipping the microelectrode into zero P_{O_2} solutions made by adding either 0.2 M $NaHSO_3$ (Davies, 1962) or buffered Ringer's solution containing 20% glucose and the enzyme glucose oxydase (Wiernsberger et al., 1976). Since these techniques gave identical results to within 0.1 pA, only the former was regularly used. Most of the microelectrodes tested had a dark current that ranged from 0.0 to 0.4 pA. When the dark current was for unknown reasons higher than that, the electrode was discarded. The electrodes used in this study were, as expected, insensitive to changes in flow (Fatt, 1976), and negligibly little oxygen was consumed by the electrode.

Preparation of the Retina

The drone was decapitated, the antennae were cut off, and the head, with the posterior surface up, was put in a concave well in a stainless steel head holder (Fig. 2 *B*): the well had been filled with a low-melting-point (37°–38°C) wax (Eicosan, Fluka A. G., Buchs, Switzerland). The orientation of the head in the well was carefully adjusted so that the dorsal part of the cornea protruded about 100 μm above the edge. Then the protruding part was sliced off with a new razor blade vibrating at 300 Hz to expose a layer of ommatidia lying flush with the floor of the chamber (Fig. 2 *B*).

Perfusion Chamber

A chamber was built fulfilling certain hydrodynamic requirements. Fig. 2 *A* is a schematic representation of this chamber. The main body is of Plexiglas. The floor is covered by a sheet of polished stainless steel, thoroughly cleaned with alcohol. The width of this chamber (40 mm) is much larger than the diameter of the drone head, and the distance from the input to the output is 80 mm. The head in its holder was fitted in a circular hole (diameter, 7 mm) in the floor of the chamber, 40 mm from the inlet. By means of a screw in the base of the hole, the upper surface of the head holder could be brought flush with the chamber floor (Fig. 2 *B*), so that turbulent flow over the head could be avoided. At the outlet of the chamber the stainless steel floor curved downward and a glass cover slip was propped against it (Fig. 2 *A*); because of this, the level of fluid remained constant to within a few micrometers over the range of flow between 0.5 and 20 ml/min. A bolus of fluorescein injected before the input of the chamber showed a parabolic profile, indicating that the flow was laminar. In addition, when the flowing fluid in the chamber was scanned with a P_{O_2} microelectrode, starting from the middle (where the retina is normally located) and going toward the sides of the chamber, the P_{O_2} was constant (for any given flow rate and depth) to within 1 mm of the sides.

Perfusion Medium

The retina was superfused with oxygenated Ringer's solution of the following composition (millimolar): NaCl, 283; KCl, 10; $CaCl_2$, 1.8; $MgCl_2$, 5; Tris-HCl, 10; pH 7.4. The Ringer's solution was pumped to the chamber by a peristaltic pump. On the

basis of experimental results, two flow rates of 8.7 and 11.2 ml/min were chosen for the measurements. Given the cross section of the chamber, it can be estimated that for these two flow rates the mean velocity of the flow is ~2 and 3 mm/s, respectively.

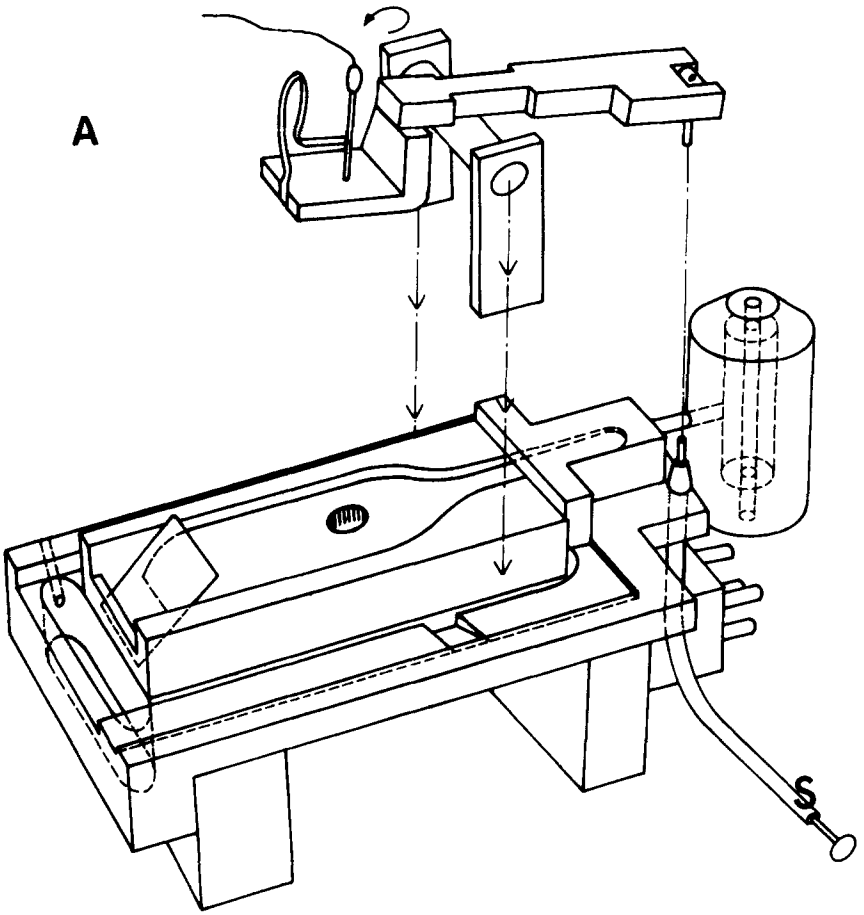

FIGURE 2. (*A*) Exploded diagram of the perfusion chamber together with the system for the measurement of *D*. When the shutter cable (*S*) is operated, the Plexiglas plate in which the surface O_2 electrode is mounted rotates, as indicated by the arrow, and covers almost the entire width of the chamber, including the retina, without leaving any visible space between the lower surface of the Plexiglas plate and the floor of the chamber (see also text). (*B*) Schematic representation of the superfused cut-head preparation seen from above. The heavy line ring represents the head holder (diameter 7 mm) in which the head is fixed by wax (*W*). The retina (*R*) of one eye is oriented so that some ommatidia are perpendicular to the lines of flow. Black arrow indicates the cornea; white arrow the basal membrane; and *B* the brain.

120 μm from the retinal surface, the estimated velocity is ~0.5 mm/s when the flow rate is 10 ml/min. Before reaching the chamber, the flow passed through a Teflon-membrane gas exchanger (Dünnschicht Dialysator, L. Eschweiler and Co., Kiel, W.

Germany). The efficiency of this oxygenator was satisfactory, because the values of P_{O_2} obtained in 100% O_2-equilibrated solutions flowing in the perfusion chamber were those expected from the calibration curves of the electrode (~703 mm Hg at 22°C in Geneva).

Movement of the Electrode and Measurement of Electrode Position

The electrode displacement was measured by a 20-turn potentiometer connected to the fine screw of a Leitz (Wetzlar, W. Germany) micromanipulator by a rubber O-

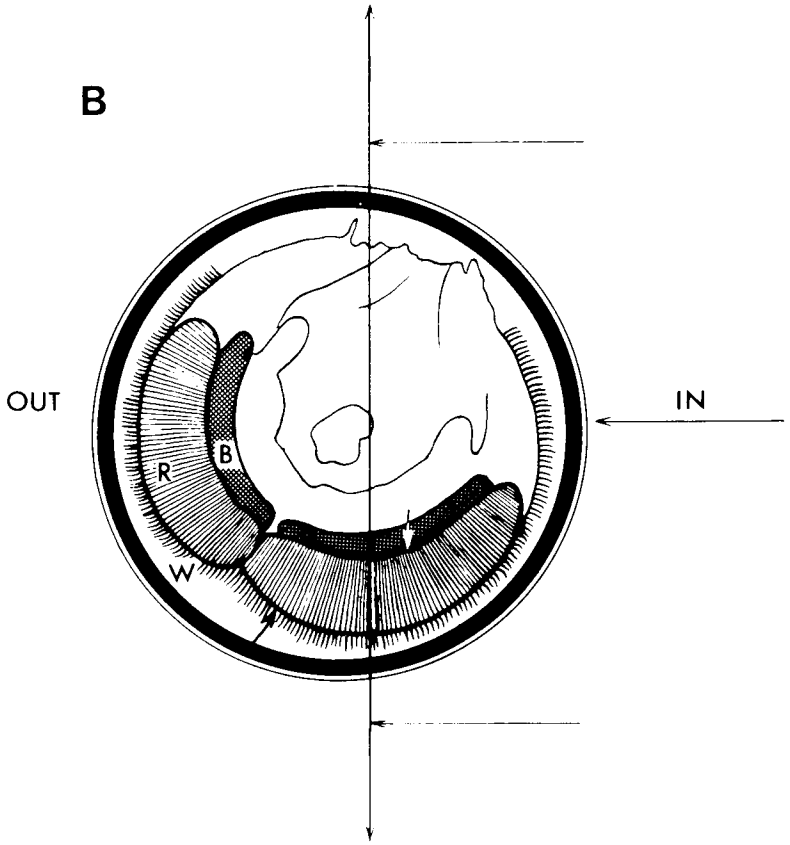

ring. For 1,000-μm movement, the total error was ~1% (10 μm). Precise step movements down to 20 μm (usually made in this study) were possible. The vertical displacement of the micromanipulator made a 60° angle with the bottom of the chamber. The electrode was advanced in a direction opposite that of the flow; this had the advantage that the tip of the electrode measured the P_{O_2} in a region undisturbed by the physical presence of the electrode.

Measurement of D

The method was similar to that described by Takahashi et al. (1966) in their determinations of D and Q in rabbit corneal stromata and by Evans and Constable (1976) in their measurements in bacterial suspensions. Basically, the method consists

of abruptly sealing the retina from the O_2 of the perfusion medium and then measuring the time required for it to consume all of its dissolved O_2. The tissue preparation and the perfusion chamber are described above. The exposed retinal surface was sealed by two methods.

METHOD I The Ringer's solution flowing over the retina was rapidly replaced by a paraffin or silicon oil by means of the pneumatic valves described by Coles and Tsacopoulos (1979). The subsequent time-course of P_{O_2} was measured by an O_2 microelectrode previously positioned below the exposed retinal surface. Various tests have revealed that these oils have a D more than 10 times lower than the water. However, since we could find no liquid completely impermeable to O_2, this method was replaced by Method II.

METHOD II A plate of Plexiglas was abruptly dropped onto the retinal surface, possibly trapping a very thin layer of fluid but no air bubble. The upper part of Fig. 2 *A* is a schematic representation of the system. The O_2 electrode consisted of a 125-μm Pt wire etched at the tip to 1 μm and insulated with shellac inside a 0.5-mm glass

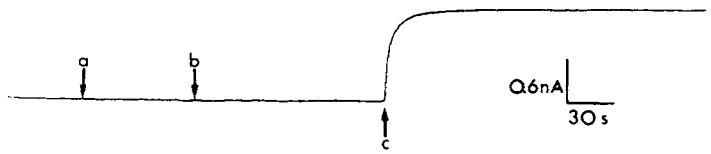

FIGURE 3. Test of sealing by the surface electrode. The surface electrode was in the chamber about 0.5 mm above the head holder (Fig. 2 *A*), the space for the retina being filled with wax. Ringer's solution equilibrated with air was flowing. The record is the oxygen current. (*a*) The electrode was dropped over the head holder. No change in the O_2 current was observed. (*b*) The perfusate was switched to a Ringer's solution equilibrated with 100% O_2. This O_2 did not reach the electrode surface. (*c*) The surface electrode was abruptly raised by a few tens of micrometers. Oxygenated Ringer's solution was now able to reach the electrode and the current increased.

capillary. The electrode was polished on a beveller until its measuring surface was ~2–3 μm^2, and, when immersed in air-equilibrated Ringer's solution, it gave a current of 1.5–2.0 nA. These electrodes usually had a linear calibration curve, and the dark current measured with the glucose oxydase technique (see above) was between 30 and 150 pA (10 electrodes). Bare electrodes were used in this study, because the fastest response time of the electrode was required. Indeed, when the O_2 electrode was covered with a polystyrene sheet as thin as 1–2 μm, even though its response time was reasonably short ($t_{90\%}$ ~1 s), the electrode was not fast enough to measure accurately the rapid drop of P_{O_2} (see Results). Theoretically, the major problem arising from the use of bare O_2 electrodes would be the stirring effect (Davies, 1962). However, this effect was relatively small (2–5%), probably due to the smallness of the sensing surface of the electrode (see Fatt [1976] p. 20). There were two other reasons for making the electrode so small: to diminish the electrode's oxygen reduction rate to a minimum and to make the measurements as local as possible (see calculations made by Takahashi et al. [1966]). The calibration curve of the electrode was not affected by its location in the Plexiglas plate, whose presence in the bath, ~1 mm from the retina, did not affect the characteristics of the P_{O_2} curve obtained with the recess-type O_2 microelectrode. Another control experiment (Fig. 3) demonstrated the effectiveness of the sealing of the retinal surface with the Plexiglas plate.

The typical experimental procedure of Method II was the following: when the P_{O_2} distribution reached a steady state (generally ~1 h after the retina was sliced) the P_{O_2} was measured with the O_2 microelectrode along an axis normal to the surface of the retina, in the bath and in the tissue. Then the Plexiglas plate (with O_2 electrode in place) was oriented under microscope control so that, when the plate was dropped over the retina, the sensing surface of the electrode tightly occluded the retina in the middle of the ommatidia at about the same place as the depth of the O_2-supplied layer had been measured. One measurement of D per retina was made.

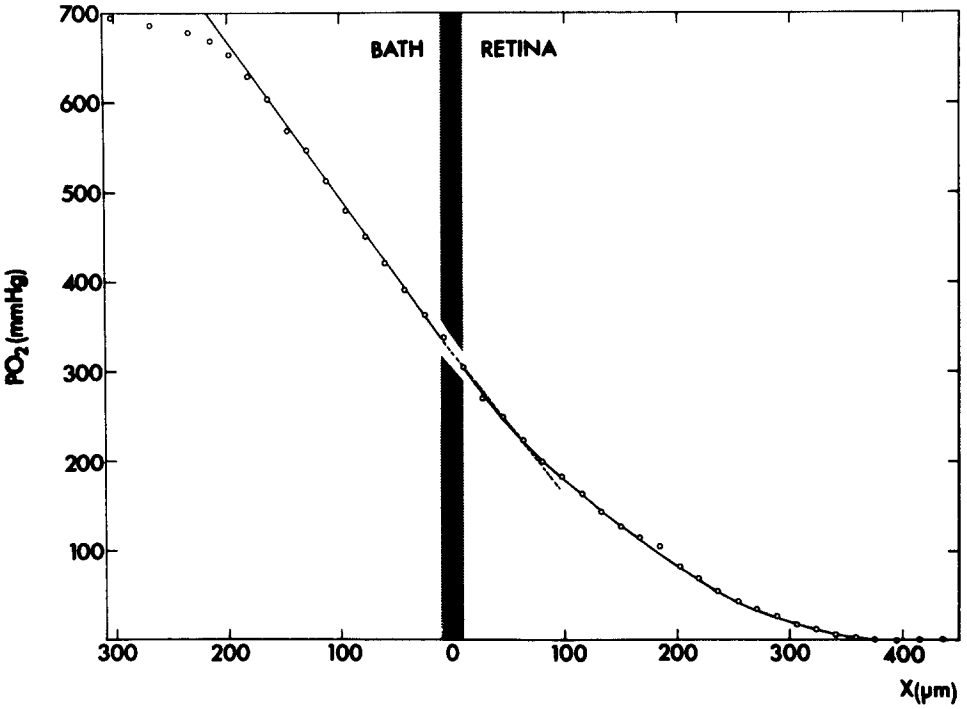

FIGURE 4. Sample recording of P_{O_2} as a function of distance (x); the position of the exposed retinal surface is indicated by zero, the bath being to the left and the retina to the right. The dotted line is the mean slope through the first five intraretinal points. It shows that the P_{O_2} gradient barely changed when the electrode passed from the bath into the retina.

RESULTS

Steady-State P_{O_2} Measurements

When the P_{O_2} microelectrode was advanced by steps of 20 μm from the bulk of the bath toward the exposed surface of the retina, P_{O_2} was constant for a long distance. The first changes appeared at ~240 μm above the retinal surface. The amplitude of the change per step increased for ~120 μm, but it remained approximately constant in the last 120–140 μm above the exposed retinal surface. This appears in the plot of Fig. 4 as a straight line. Inside the tissue, P_{O_2} values decreased as a function of depth and reached zero ~400 μm from the surface. Ganfield et al. (1970) have obtained a similar curve in

experiments made on superfused brain slices, and they concluded that the straight part of the curve indicates the existence of a boundary layer equivalent to 40 μm of nonflowing solution. Since their calculations depend on the important assumption that in the boundary layer transport is only perpendicular to the surface, we decided to explore this in detail.

Theory

The geometry of the system is presented schematically in Fig. 5. Symbols x, y, and z denote the three space-coordinate axes: x is perpendicular to the exposed

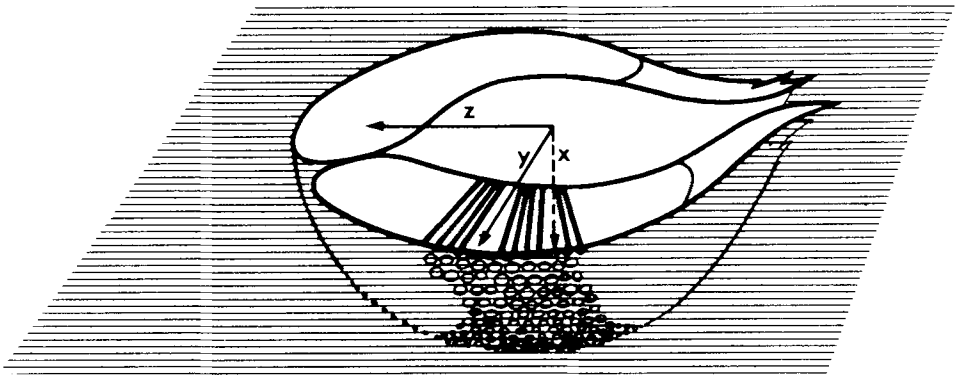

FIGURE 5. Schematic representation of the cut-head preparation, to facilitate the understanding of the theoretical analysis. The perfusate flows along the axis z while some of the ommatidia are lying almost along the axis y. The cornea (some facets are indicated by circles) is practically impermeable to O_2, but in spite of that, in the experiments, the eyes were surrounded by wax (hatched area; see also Methods). The experimental evidence suggests that the O_2 diffuses only along the axis x, i.e., from the bath to the retina.

surface of tissue and z is the direction of flow of the perfusion medium. In the experimental conditions of this study (Fig. 5), there are at least three factors affecting the concentration of O_2 in the system, namely, (*a*) diffusion of the free oxygen molecules, (*b*) transfer of molecules resulting from the convective flow in the bath, and (*c*) chemical reactions consuming O_2. Consequently, the local concentration of free oxygen, $C(\vec{r},t)$, will change according to the equation (see, e.g., Levich [1962])

$$\frac{\partial C}{\partial t} = \nabla\cdot(D\nabla C) - \vec{V}\cdot\nabla C - Q. \tag{1}$$

Or, replacing C with αP,

$$\frac{\partial(\alpha P)}{\partial t} = \nabla\cdot[D\nabla(\alpha P)] - \vec{V}\cdot\nabla(\alpha P) - Q, \tag{2}$$

where ∇ is the differential operator $\left(\frac{\partial}{\partial x};\frac{\partial}{\partial y};\frac{\partial}{\partial z}\right)$, $\vec{V}(\vec{r},t)$ the vector field

describing the collective movement of the medium, P the P_{O_2}, D the diffusion coefficient, and α the solubility coefficient of oxygen in the medium.

For the present experimental conditions, Eq. 2 can be simplified using reasonable assumptions, namely, that D and α are constant with values D_B and α_B in the bath, and D_R and α_R in the retina; that the x and y components of $\vec{V}$ are negligible (laminar flow, see Methods); and that, since the chamber is much wider than the preparation, V_z is independent of y and z over the retina.

Under these conditions and since $Q = 0$ in the bath and $\vec{V} = \vec{0}$ in the tissue, Eq. 2 becomes

$$\frac{\partial P}{\partial t} = D_B \nabla^2 P - V_z \frac{\partial P}{\partial z} \tag{3 a}$$

in the bath and

$$\frac{\partial P}{\partial t} = D_R \nabla^2 P - \frac{Q}{\alpha_R} \tag{3 b}$$

in the retina.

Using these equations together with the equation given by the continuity of the diffusion flux $-D\alpha(\partial P/\partial x)$ across the interface, it is possible to estimate the values of Q, α_R, and D_R, provided the values of P, V_z, D_B, and α_B are known. We found it suitable for our experiments to consider two situations: (*a*) when steady state is reached and (*b*) when the interface is suddenly occluded with an impermeable boundary (interruption of oxygen exchange at the interface).

STEADY STATE $[(\partial P/\partial t) = 0]$ The exact resolution of Eqs. 3 *a* and 3 *b* depends on the boundary conditions applying to the system. Instead of chosing arbitrary boundary conditions for the steady state, we decided to measure the values of $\partial P/\partial y$ and $\partial P/\partial z$ over the retina (see below). We found them to be vanishingly small compared with $\partial P/\partial x$, thus indicating that: (*a*) the one-dimensional model can satisfactorily describe the diffusion of O_2 in the superfused retina; (*b*) Q does not noticeably vary, on the macroscale, along the axes y and z in the retina; and (*c*) since V_z vanishes at the surface of the retina, there is a region in the bath, close to the retina, where the term $V_z(\partial P/\partial z)$ can be neglected.

Thus, Eqs. 3 *a* and 3 *b* become

$$D_B \frac{\partial^2 P}{\partial x^2} = 0 \tag{4 a}$$

in the bath close to the retina and

$$\frac{\partial^2 P}{\partial x^2} = \frac{Q}{\alpha_R D_R} \tag{4 b}$$

in the retina.

The solutions of Eqs. 4 *a* and 4 *b* are a straight line in the bath, and in the

retina a curve with a shape that depends on the value of $Q/\alpha_R D_R$. Since both solutions are linked by the conditions of continuity of the flux and of P, it is possible to infer from them the mean value of $Q(\bar{Q})$ together with the value of the product $\alpha_R D_R$, as we show below, provided the values of α_B and D_B are known.

Since the one-dimensional model applies over the major part of the retina and since the flux (F) normal to the interface is only due to diffusion, the O_2 flux entering the retina has the following value:

$$F = \alpha_B D_B \Delta \tag{5}$$

where $-\Delta$ is the slope of the straight line in the bath (Fig. 4). Consequently, the mean value of Q in the oxygenated part of the retina is

$$\bar{Q} = \frac{F}{l} = \frac{\alpha_B D_B \Delta}{l}, \tag{6}$$

where l is the depth of tissue supplied with O_2.

If Q is uniform throughout the consuming tissue, P is a parabolic function of x (Hill, 1928), so that the plot of $\sqrt{P}$ vs. x is a straight line with a slope γ given by (see Appendix):

$$\gamma = -\sqrt{\frac{Q}{2\alpha_R D_R}}. \tag{7}$$

Thus, using Eqs. 6 and 7, we find for $\alpha_R D_R$:

$$\alpha_R D_R = \frac{Q}{2\gamma^2} = \frac{\alpha_B D_B \Delta}{2\gamma^2 l}. \tag{8}$$

As we show in Appendix, the same results apply to certain other cases of $Q(x)$, provided that Q is replaced by $\bar{Q}$.

OCCLUSION OF THE INTERFACE AFTER STEADY STATE The one-dimensional expression of Eq. 3 *b* is

$$\frac{\partial P}{\partial t} = D_R \frac{\partial^2 P}{\partial x^2} - \frac{Q}{\alpha_R}. \tag{9}$$

When the flux of oxygen through the interface is abruptly stopped, if Q is independent of P, Eq. 9 turns into a moving boundary problem, the resolution of which is difficult. However, the particular case of uniform Q has been investigated in detail by Crank and Gupta (1972). They showed that (*a*) the depth of the oxygenated layer changes very little at first and then abruptly comes to zero when all the available oxygen has been consumed in the tissue and (*b*) the exact value obtained numerically for the time-course of P at the interface, $P_o(t)$, is very closely fitted by the following expression:

$$P_o(t) \cong P_o(0) \cdot \left[1 - \sqrt{\frac{16 D_R}{\pi l^2}} \cdot \sqrt{t}\right] \tag{10}$$

According to Eq. 10, a plot of P_o versus $\sqrt{t}$ should yield a straight line. In

this way, calling t_o the time at which P_o comes to zero and using Eq. 10, we can estimate D_R from the following equation

$$D_R = \frac{\pi l^2}{16 t_o}. \tag{11}$$

In conclusion, since we already know from Eqs. 6 and 8 the values of $\bar{Q}$ and $\alpha_R D_R$, we have a method of estimating $\bar{Q}$, D_R, and α_R from P_{O_2} recordings in the cut-head preparation.

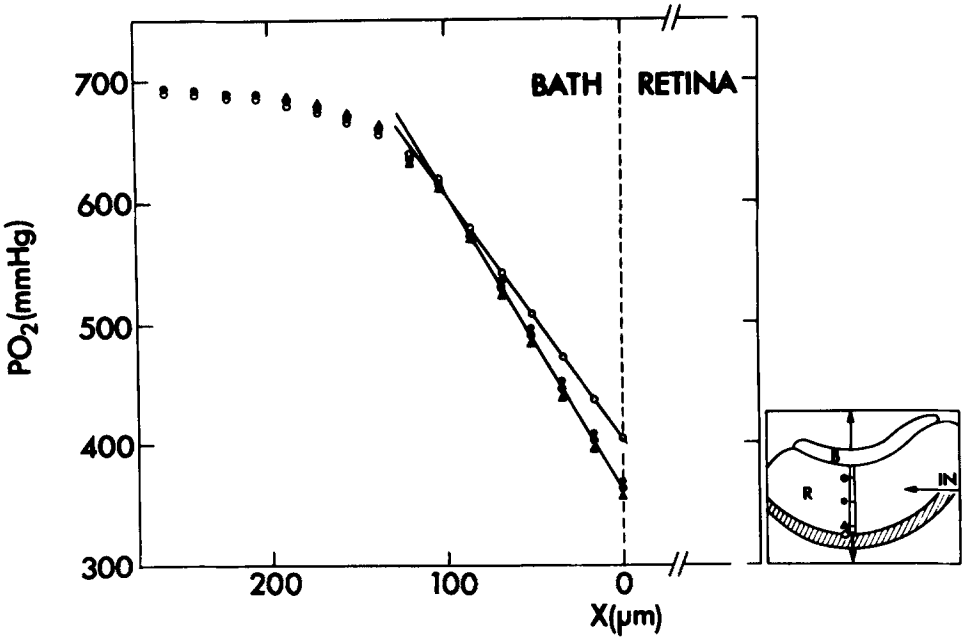

FIGURE 6. Measurement of $P(x)$ in the bath at different positions along the axis y. In the scheme presented in the *inset* the positions are indicated by different symbols: ○, position 1; ▲, position 2; *, position 3; and ●, position 4. In these experiments the ommatidium was oriented perpendicular to the lines of flow.

Validity of the One-dimensional Model

Eqs. 6, 8, and 11 are valid only if Q does not vary on the macroscale along the y and z axes in the retina and P is independent of y and z in the retina and over it. This has been tested by recording P at different sites along the exposed retinal surface in the steady state.

The *insets* of Figs. 6 and 7 show schematically the experimental protocol followed in these experiments. First, measurements were made at four sites along the y axis, i.e., the length of a given ommatidium situated in the middle of the eye and oriented perpendicularly to the direction of the lines of flow. Fig. 6 shows a sample experiment, and Table I summarizes the values of Δ and P_o obtained from eight experiments at sites 1–3. Δ was lower at the

pigmented zone of the ommatidium close to the cornea (site 1) than in the remaining sites along the ommatidium. In contrast, there was no significant difference between the slope measured ~50μm proximal to the pigmented zone of the ommatidium (site 2) and sites 3 and 4. P_o was somewhat more variable, but there was virtually no difference among sites 2–4. However, there was a small but clear difference between site 1 and the other sites along the axis of the ommatidium, P_o being higher close to the cornea. This phenomenon could be due to a lower oxygen consumption locally at the level of the pigmented zone of the ommatidium or to the transition from consuming to nonconsuming regions of the chamber. In the presence of this ambiguity, the experiment was repeated but with the ommatidium oriented parallel to the lines of flow with the corneal part of the ommatidium situated downstream. Even under these conditions, P_o was lower at site 3 than at site 1 and Δ was higher at site 3 than at site 1. Qualitatively identical results were obtained in six retinas.

TABLE I

MEASUREMENT OF P_o AND Δ ALONG THE y AXIS

	P_o			Δ		
Exp.	Posit. 1	Posit. 2	Posit. 3	Posit. 1	Posit. 2	Posit. 3
		mm Hg			*mm Hg/μm*	
1	400	381	380	1.52	1.85	1.85
2	410	396	367	1.60	1.75	1.66
3	425	365	360	1.60	1.94	1.94
4	412	380	370	1.67	2.15	2.12
5	396	313	307	2.25	2.55	2.55
6	410	310	308	1.51	2.35	2.29
7	455	405	396	1.55	1.82	1.85
8	461	392	383	1.60	2.20	2.20
$\bar{X}$	421.1	367.7	358.9	1.66	2.08	2.05
SD	±24.4	±36.7	±33.6	±0.24	±0.28	±0.28
SEM	±8.6	±13.0	±11.9	±0.09	±0.10	±0.10

Consequently, we conclude that the pigmented region of the ommatidium has a lower Q than the rest of the ommatidium. This finding fits with the histology, which shows that at the pigmented part of the ommatidium the pigment cells (which have few mitochondria) have a much larger volume than the mitochondria-rich photoreceptors (Perrelet, 1970). However, the important finding is that along the greatest part of the y axis over the retina, P was practically constant, i.e., $\partial P/\partial y \simeq 0$.

In other experiments, the exposed retinal surface was scanned with the microelectrode along the z coordinate, the ommatidia being oriented perpendicularly to the lines of flow (*inset* of Fig. 7). As shown in Fig. 7, there was negligible variation of Δ and P_o over a large part of the z axis, so that $\partial P/\partial z \simeq 0$. In addition, in four experiments, $P(x)$ was measured at two or more sites inside the retina. The curves from each retina were almost indistinguishable, the oxygenated depth being the same to within 20 μm.

In conclusion, $\partial P/\partial y$ and $\partial P/\partial z$ are negligible in the region of interest, justifying the use of Eq. 6.

Measurement of Q and Permeation Constant $\alpha_R D_R$

Fig. 8 shows on an expanded scale the right part of Fig. 4, as well as a plot of $\sqrt{P(x)}$. As expected from Eq. A5 (Appendix), this plot is closely fit by a straight line, so that we can consider Q as uniform inside the tissue. Consequently, it is possible to use Eqs. 6 and 8 to estimate Q and $\alpha_R D_R$. The results of 10 experiments are presented in Table II. The pooled value of Q was 18 ± 0.7 (SEM) μl O_2/cm^3 tissue·min. Using the value 3.32×10^{-5} ml O_2/cm · atm · min for $\alpha_B D_B$ (Goldstick and Fatt, 1970; Altman and Dittmer, 1971),

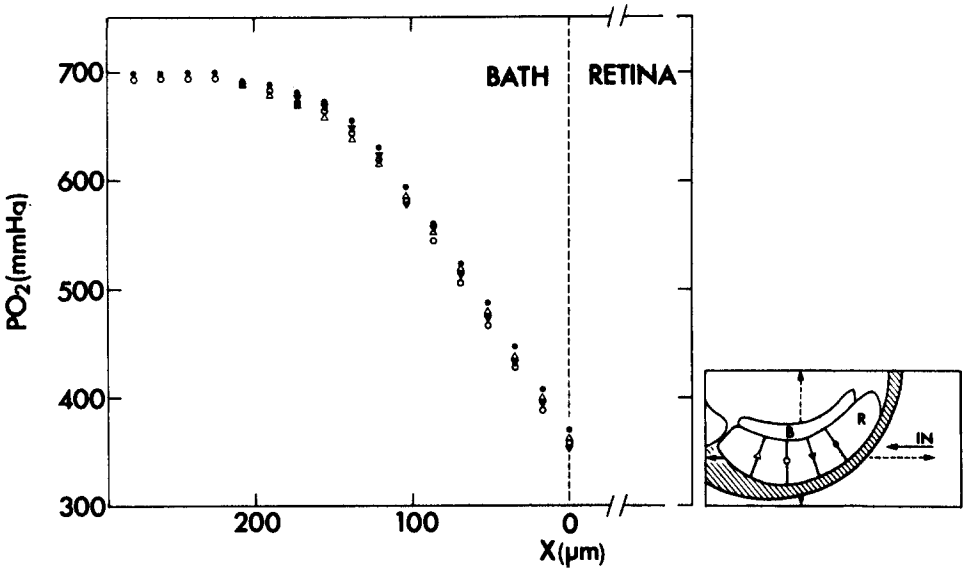

FIGURE 7. Measurements of $P(x)$ in the bath along the axis z at a position corresponding to the middle of the ommatidium (site 3 of Fig. 6). *Inset* shows the experimental protocol and the corresponding symbols. Distance between the two extreme sites (Δ and *) was ~1 mm.

the value obtained for $\alpha_R D_R$ was 3.24 ± 0.18 (SEM) $\times 10^{-5}$ ml O_2/min·atm·cm, i.e., very close to that reported for pure water. In 10 other experiments, Q, measured under a perfusion flow of 8.7 ml/min, was very close to that measured under 11.5 ml/min (see Table III).

Immediately after the head was sliced to expose the ommatidia and starting perfusion, the slope $-\Delta$ was steep, but it progressively decreased until a steady value was reached. Usually, with 100% oxygenated Ringer's solution and in darkness, it took ~1 h of perfusion to reach a steady value of Δ. This value remained stable at a given location of the retina and in good preparations for up to 6 h. The values of Q presented in Tables II and III were obtained at between 1 and 5 h of perfusion and dark adaptation and from tissue penetrations made exclusively in the middle of the ommatidia.

In some experiments, the plot $\sqrt{P}(x)$ was fitted by a linear regression as satisfactorily as in Fig. 8. In other cases, there were conspicuous periodic fluctuations around the straight line (Fig. 9 *A*). We show in the Appendix that if this arises from periodic fluctuations in Q related to the structural heterogeneity of the drone retina (Fig. 12), then the results of the analysis are

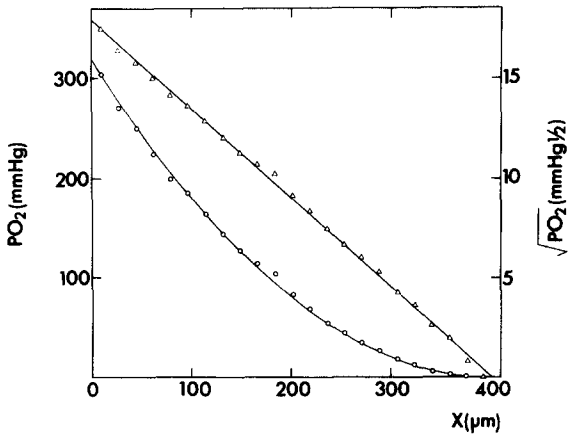

FIGURE 8. Shows the right part of the Fig. 4 (intraretinal) on an expanded scale (○). The straight line (△) is a plot of $\sqrt{P}(x)$. Zero distance corresponds to the exposed retinal surface. The solid, straight line is the best linear fit of $\sqrt{P}$, and the corresponding value of $P(x)$ is indicated by the solid curve.

TABLE II

VALUES OF Q, αD, D, AND α

Exp.	Δ	l	$-\gamma$	t_o	Q	$\alpha D \cdot 10^5$	$D \cdot 10^5$	α
	mm Hg/ /μm	*μm*	*mm Hg$^{1/2}$/ /μm*	*s*	*μl O$_2$/ /cm^3· min*	*ml O$_2$/ /cm·atm·min*	*cm^2/ /s*	*μl O$_2$/ /cm^3·atm*
1	2.024	478	0.041	39	18.5	4.16	1.15	60
2	1.826	414	0.050	32.5	19.3	2.94	1.04	47
3	1.520	526	0.038	45.5	12.6	3.35	1.19	47
4	1.720	430	0.048	26.5	17.5	2.85	1.37	35
5	1.539	386	0.051	40.5	17.4	2.60	0.72	60
6	2.041	456	0.043	35	19.6	4.01	1.17	57
7	2.122	440	0.049	40	21.1	3.32	0.95	58
8	1.426	368	0.053	40	16.9	2.31	0.67	58
9	1.670	392	0.045	40	18.6	3.53	0.75	78
10	1.733	434	0.045	29.5	17.4	3.28	1.25	44
$\bar{X}$					17.9	3.24	1.03	54
SEM					±0.7	±0.18	±0.08	±4.0

still valid. In still other experiments, after a depth of ~300 μm, there was a significant deviation from the expected straight line (Fig. 9 *B*). A number of explanations can be proposed to account for this, e.g., decreased Q at low P_{O_2} (Hill, 1948), facilitated diffusion (Wyman, 1966; Ganfield et al., 1970), or, less probably, changes in electrode sensitivity. To calculate Q in such cases,

the straight portion of the curve was extrapolated to zero, and the distance thus obtained was used for the estimation of Q (see also Gore and Whalen [1968]). As shown in Table III, the mean Q calculated from complete linear plots of $\sqrt{P}$ vs. x is the same for all three cases.

Measurement of D in the Dark-adapted Retina

From the steady-state measurement of P inside the tissues, we have concluded that Q is uniform (perhaps with a slight periodicity). Therefore, the value of P at the interface, $P_o(t)$, is expected to change according to Eq. 10 from the moment when the surface is occluded. The method used for this study is described in Methods. Fig. 10 shows a sample recording of the electrode current as a function of time: the ordinate is labeled with P_{O_2} values obtained from calibration of the electrode. The P_{O_2} fell in two distinct phases, (the transition is indicated by the dotted line in Fig. 10). The first phase corresponds to the rapid drop of P_{O_2} from the value existing in the bath to about the value

TABLE III

CONSUMPTION UNDER DIFFERENT CONDITIONS

Q			
A	B	C	D
$\mu l\ O_2/cm^3\ tissue \cdot min$			
20±2.0 SE $n = 10$	18±0.7 SE $n = 10$	20±0.9 SE $n = 15$	20±1.0 SE $n = 15$

A, under a flow rate of superfusion of 8.7 $ml \cdot min^{-1}$.
B, under a flow rate of superfusion of 11.5 $ml \cdot min^{-1}$. $\sqrt{P(x)}$ was a straight line.
C, $\sqrt{P(x)}$ was a straight line for more than 300 μm, but deviated at low P. The total O_2-supplied depth was taken for the estimation of Q.
D, same as *C*, but the straight portion of the curve was extrapolated to zero, and the distance thus obtained was used for the estimation of Q.

of P_o. During the second phase, the current fell slowly to zero. In this particular record, after the completion of sealing, the retina took about 1 min to consume all its O_2 store. Eq. 10 predicts that a plot of P_o vs. $\sqrt{t}$ should be a straight line with slope $-\sqrt{\frac{16D_R}{\pi l^2}} \times P_o(0)$. Such a plot is made in Fig. 11 with selected values taken on the recording of Fig. 10 starting from the moment of the appearance of the mechanical artifact ($t = 0$) and continuing to the end of the first oscillographic sweep. The straight line of Fig. 11 has been calculated by linear regression using values taken between the arrows. In this range the experimental points lie on the straight line, but deviations appear at the beginning and at the end of the graph. Possible explanations for these deviations are given in the Discussion.

The data from 10 retinas (one run per retina) at 21.6°C are shown in Table II. In all these experiments, the plot of P_o vs. $\sqrt{t}$ was at least as linear as the one presented in Fig. 11, and the $\sqrt{P(x)}$ inside the retina, determined with the recess electrode before the sealing of the exposed surface, gave approximately

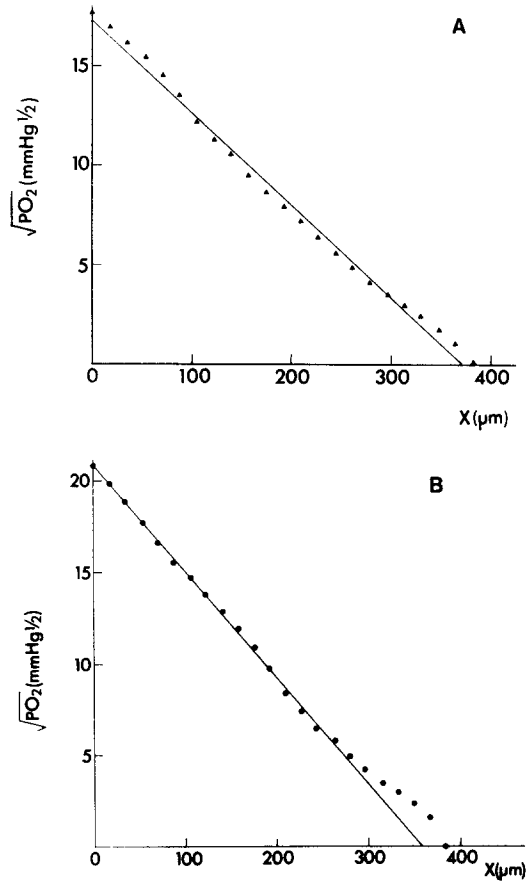

FIGURE 9. Plots of intraretinal $\sqrt{P}(x)$ vs. x, as in Fig. 8, showing typical deviations from linearity.

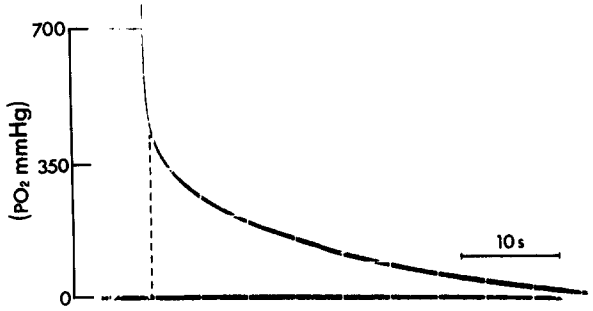

FIGURE 10. Oscilloscope record of P_{O_2} change as a function of time after sealing of the exposed retinal surface from the O_2 source with the Plexiglas plate. The mechanical artifact (upward deflexion of the O_2 current) indicates the moment at which the Plexiglas plate was pushed toward the retina. The dashed line indicates the transition from the rapid phase to the slow phase of the fall of P_{O_2}.

a straight line, indicating an almost uniform Q and the existence of one-dimensional diffusion. The mean value of D_R calculated from Eq. 11 was 1.03 ± 0.08 (SEM) × 10^{-5} cm^2/s. The variability of the individual results listed in Table II is perhaps due to the relative imprecision of the measurements of t_o from one experiment to another.

Only five experiments were carried out with paraffin oil, for the reasons

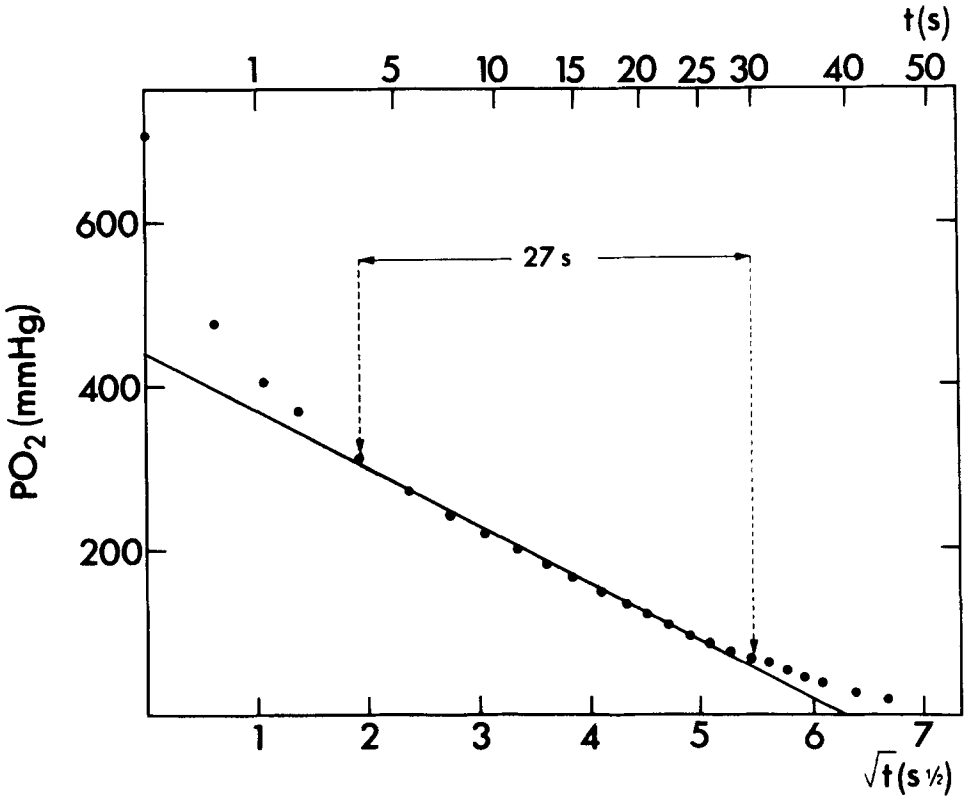

FIGURE 11. Plot of the values of P_{O_2} taken from the recording of Fig. 10 as a function of square root of time. The solid line is the best linear fit of the recorded values of P_{O_2} taken between the two arrows. The calculated straight line is that predicted by the model of Crank and Gupta (1972) (see Theory). The x intercept of the straight line gives the value of t_o, which is introduced into Eq. 11 to calculate D.

given in Methods. The fit of these data by Eq. 10 was less satisfactory than when the retina was sealed with the Plexiglas plate, but the best estimate of D, 1.0 × 10^{-5} cm^2/s, was similar.

The values of the solubility coefficient α_R were derived in each experiment from the estimates of $\alpha_R D_R$ and D_R, and they are listed in Table II. The mean value obtained for α_R was then 54 ± 4.0 (SEM) μl O_2/cm^3 tissue·atm, which is ~80% higher than in pure water at the same temperature (International Critical Tables).

DISCUSSION

The aim of this study was to obtain values of the steady-state rate of O_2 consumption (Q), and the diffusion (D) and solubility (α) coefficients to be used later in a quantitative determination of the kinetics of Q after a single flash of light. In control experiments P_{O_2} was measured at different sites in the bath and in the retina, and it was found that the P_{O_2} at the exposed retinal surface (P_o) and the magnitude of the O_2 flux (F) entering the retina perpendicularly to this surface were practically uniform over the whole superfused retina, a situation that greatly simplified the analysis. *A priori* we did not expect this: the theoretical analysis made by Levich (1962) of a system in which a solution flows over an infinite plane absorbing surface, suggested that along the z axis, at least, P_o would be higher close to the inflow than, for example, in the middle of the retinal surface. The experiments showed, however, that P_o and F are constant in the x-y plane, presumably because the retina is narrow compared with the width of the chamber and balance flux occurs from the borders and because along the y axis the high retinal Q contributes to the rapid establishment of uniform P_o and F. In this study, the exact mathematical solution of the curve $P(x)$ in the bath was not pursued, because the precise distribution of the velocities of the fluid along the axis x was not measured. This, however, does not invalidate the results presented here.

A second major simplification was discovered: Q was essentially constant in the retina down to P_{O_2}s <20 mm Hg. This finding agrees with those of Gore and Whalen (1968) from work in muscle and Ganfield et al. (1970) from work in mammalian brain slices. However, when the fine structure of the drone retina is considered, it might be expected that Q would not be the same everywhere. The mitochondria where Q occurs are aligned along the periphery of the photoreceptor cells, which in turn are surrounded by the mitochondria-free glial cells. From this mitochondrial distribution one would expect the Q distribution to be roughly periodic (see Fig. 12 in Appendix). However, the mathematical analysis given in the Appendix shows that the retinal Q, on the macroscale, will appear as uniform because $\sqrt{P(x)}$ is always close to a straight line.

Q in Darkness

The value of Q of the completely dark-adapted drone retina appears high compared, for example, with the values of resting sartorius muscle at 20°C (Mahler, 1978*a*) or the corneal stroma (Takahashi et al. 1966). Using a microtechnique similar to ours, Ganfield et al. (1970), obtained in mammalian brain slices at 37°C a value of 89.8 μl O_2/cm^3 tissue·min. Assuming $Q_{10} = 2$ for the drone retina (Autrum and Hamdorf, 1964), our value of Q for the drone retina appears only a little lower than that of mammalian cerebral cortex. More relevant, however, are the values obtained by Hamdorf and Kaschef (1964) using a micro-Warburg manometric technique. They found the retinal Q of flies (*Calliphora erythrocephala*) maintained in darkness to be ~60 μl O_2/cm^3 tissue·min at 22°C, or about threefold higher than in drones.

For the worker bee, Autrum and Hamdorf (1964) give the oxygen consumption per *eye*: if the weight of the retina is taken as 0.5 mg (our unpublished measurement) their figure corresponds to a Q of 40 μl O_2/cm^3 tissue·min (at 22°C). In most of our experiments, the retina was allowed to dark adapt for at least 1 h. In preliminary experiments, Q was measured after only 10–15 min of dark adaptation after a prolonged illumination with continuous light, and the value was 35 ± 8.0 (SEM) μl O_2/cm^3 tissue·min (n = 6), i.e., about twice as high as the value obtained under complete dark adaptation. Hence, the value obtained by Autrum and Hamdorf (1964) is close to the value for partially dark-adapted drones.

Considering the value of retinal oxygen consumption obtained in this study, the following question arises: which are the cellular metabolic processes operating in darkness that use this energy produced by the mitochondria? Taking a mean Q = 20 μl O_2/cm^3 tissue·min (see Table III) and considering that near the middle of the ommatidia the photoreceptors occupy about two-thirds of the cellular volume of the drone retina and that they are the only element of the retina containing significant numbers of mitochondria, we obtain Q = 30 μl of O_2/cm^3 of photoreceptor·min. Assuming that the generally accepted stoichiometry P/O = 3 is also valid for the drone mitochondria, a production of 8.04 μmol of ATP/cm^3 of photoreceptor·min would be expected. There is now general agreement that the stoichiometry 3 Na^+/ATP roughly applies to (Na^+ + K^+)-ATPases (Harris et al., 1980). Therefore, if all consumption were used for the work of the pump, 24.1 μmol of ion/cm^3 of photoreceptor·min would be pumped. The resting Na^+ flux in the invertebrate retina is not known, but taking into account measurements made by means of radioisotopes in another excitable tissue, the vagal nerve of rabbit (Rang and Ritchie, 1968) and correcting for the different surface:volume ratio (Coles and Tsacopoulos, 1979), a "leaking" ionic movement of 3.45 μmol/cm^3 photoreceptor·min would be expected. This value is far smaller than that which would be obtained if all Q were used for basal pump work, and, consequently, it would appear that only a small fraction of the total energy produced by the basal Q is used for the work of the pump in darkness. Presumably, anabolic processes operating in the photoreceptors in darkness, such as synthesis of proteins, use part of the total energy production of the cell: there is biochemical and autoradiographic evidence that the drone photoreceptors, like other invertebrate photoreceptors, synthesize appreciable amounts of proteins (presumably mainly opsin) in darkness (Pepe and Baumann, 1972; Perrelet, 1972; Burnel et al., 1970; Stein et al., 1979).

Diffusion Coefficient

In the experiments in which D was measured by occluding the surface of the retina, the time-course of the decrease in P_{O_2} at the surface shows a greater deviation from linearity than is predicted by the theory of Crank and Gupta (1972). Presumably, the experimental situation differed from the ideal theoretical case, and two factors that may have played a role were (*a*) the oxygen consumption of the electrode and (*b*) the existence of a layer, perhaps only a

few micrometers thick, of Ringer's solution or nonconsuming tissue, between the electrode surface and the consuming retina. Evans and Gourlay (1977) have made numerical calculations of the effects of these factors on the P_{O_2} decay curve. In the cases they consider, they found that the curve deviates from linearity at short and long times in a way qualitatively similar to our results. At long times a deviation from linearity in the direction observed would also arise if Q became smaller at very low P_{O_2}s. It would appear, therefore, that we can satisfactorily account for the form of the experimental curve. As far as the precision of the value of D reported here is concerned, the work of Evans and Gourlay (1977) does not provide specific information. However, a rough calculation suggests that the presence of a nonconsuming layer, 10 μm thick (probably not detectable by microscope inspection), would not affect the value of D by more than 10%, although it could account for the deviation from linearity. It is relevant that the value of D found in the experiment with the paraffin oil was very close to that obtained by occluding the surface with the Plexiglas plate.

The mean value found for D in the retina at 21.6°C was 1.03×10^{-5} cm^2/s, about half the value in water. This result may be compared with those of Goldstick and Fatt (1970), who show curves of D in solutions of bovine serum albumin and of hemoglobin as functions of protein concentration. The drone retina contains 47.5 g protein/100 ml retina (mean value from 140 measurements, unpublished observation), and the observed value of D lies between the values for the solutions of the two proteins studied by Goldstick and Fatt (1970) at the same concentration. It seems likely, therefore, that oxygen diffuses through the retina less readily than through water mainly because of the presence of protein molecules. The same conclusion was reached by Mahler (1978 *a*, and 1981), whose value obtained in sartorius muscle (1.08×10^{-5} cm^2/s at 22.8°C) agrees with that expected from the theory of Wang (1954) for diffusion through protein solutions.

Solubility Coefficient

From the experiments giving D and αD, α was found to be 54 μl O_2 STP/cm^3·atm (21.6°C), ~1.8 times that for water (30.4 μl O_2 STP/cm^3·atm at 21.6°C; Altman and Dittmer, 1971). We appear to be the first to establish a value of α, for an intact tissue, greater than that for water (cf. Ganfield et al. [1970]). Indeed, many authors have assumed that α is smaller in tissues than in water because of the space occupied by proteins that are assumed to exclude oxygen (Hill, 1948; Takahashi et al., 1966; Zander, 1976). A possible explanation for the high value of α in drone retina is that a substantial part of the oxygen is dissolved in lipids, a possibility also mentioned for muscle by Mahler (1978 *a*). The value we find is equal to that of an emulsion containing 30% olive oil (for 100% oil, α = 116 μl O_2 STP/cm^3·atm (Battino et al., 1968). The lipid content of drone retina is unknown, but, since the dry weight including proteins and glycogen is 30% of the wet weight, the lipids present would have to have an α much higher than that of olive oil to account for the overall α. Thus, other factors must be invoked. One possibility might be the presence of gas in the tracheoles. However, the tracheoles extend only about halfway up

the ommatidia from the basal membrane (Perrelet, 1970), and the same value of α was obtained from measurements made at different positions along the ommatidium. Furthermore, we have never observed the tracheoles in our cut-head preparations, even though they are described as being readily visible when filled with gas rather than liquid (Wigglesworth, 1931). It would appear that some other factor, such as adsorption of oxygen on membranes or proteins, contributes to the high value of α.

APPENDIX

Generalization of Eq. 7 (See Results)

When the conditions of continuity of P and of the flux $\left(-D\alpha\frac{dP}{dx}\right)$ are considered, the solution of the steady-state one-dimensional equations

$$\begin{aligned} &\frac{d^2P}{dx^2} = 0 \qquad \text{if } x < 0 \qquad \text{(in the bath)} \\ &\frac{d^2P}{dx^2} = \frac{Q}{\alpha_R D_R} \qquad \text{if } x \geq 0 \qquad \text{(in the tissue)} \end{aligned} \tag{A1}$$

is found to be

$$P(x) = \begin{cases} P_o - \Delta \cdot x & \text{if } x < 0 \\ P_o - \dfrac{\alpha_B D_B \Delta}{\alpha_R D_R} x + \dfrac{1}{\alpha_R D_R} \displaystyle\int_0^x (x-u)\cdot Q(u)\, du & \text{if } x \geq 0 \end{cases} \tag{A2}$$

if $x \geq 0$ (all symbols are defined in Theory).

Moreover, if the diffusion flux vanishes in the tissue at some depth $x = l$, we have

$$\Delta = \frac{1}{\alpha_B D_B}\int_0^l Q(u)\, du = \frac{\bar{Q}l}{\alpha_B D_B}. \tag{A3}$$

In the case of a tissue with an anoxic core and when Q is constant in the oxygenated region ($0 \leq x \leq l$), Eqs. A2 and A3 yield the particular result:

$$P(x) = \begin{cases} \dfrac{Ql^2}{2\,\alpha_R D_R} - \dfrac{Ql}{\alpha_B D_B} x & \text{if } x < 0 \\ \dfrac{Q}{2\alpha_R D_R}(l-x)^2 & \text{if } 0 \leq x \leq l \end{cases} \tag{A4}$$

Inspection of Eq. A4 shows that in such a case the following relations must hold:

$$\sqrt{P} = \sqrt{\frac{Q}{2\alpha_R D_R}}(l-x) \qquad \text{if } 0 \leq x \leq l \tag{A5}$$

$$\frac{P_o - P}{x} = \frac{Q}{2\alpha_R D_R}(2l-x) \qquad \text{if } 0 \leq x \leq l \tag{A6}$$

We now examine briefly what happens to relations A5 and A6 when $Q(x)$ is not

constant. Using the identity

$$\frac{d^2P}{dx^2} = 2\left(\frac{d\sqrt{P}}{dx}\right)^2 + 2\sqrt{P}\frac{d^2\sqrt{P}}{dx^2} = 2\gamma^2 + 2\sqrt{P}\frac{d\gamma}{dx} \qquad \text{A7}$$

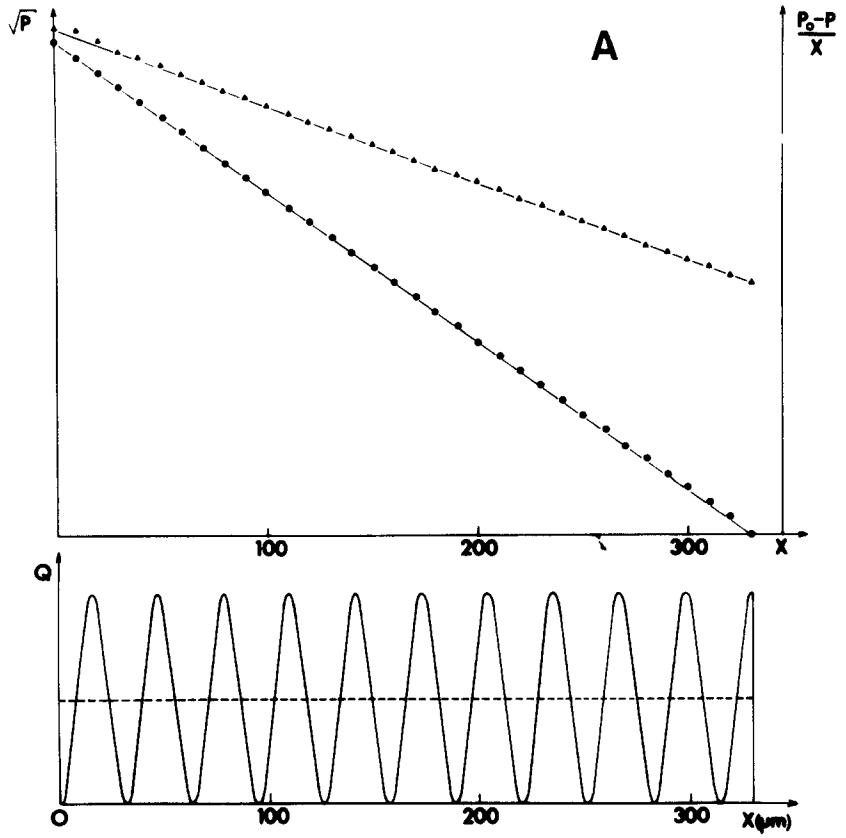

FIGURE 12. (*A*) Calculated values of P (●) and $(P_o - P)/x$ (▲) when Q is a periodical function of depth x, as shown at the bottom of the figure. These values are plotted on an arbitrary scale. Solid lines indicate the values of $\sqrt{P}$ and $(P_o - P)/x$ obtained when Q is constant. (*B*) Schematic presentation of a cross section of the drone retina: the flowerlike structures are the photoreceptors and the blank space between them is occupied by the glial cells. The O_2-consuming mitochondria (indicated by dots) are oriented at the periphery of the cells close to the cytoplasmic membrane (see Perrelet, 1970 and 1972).

together with Eq. A1, we get

$$\gamma^2 = \frac{Q}{2\alpha_R D_R} - \sqrt{P}\frac{d\gamma}{dx}. \qquad \text{A8}$$

If the value of γ does not change (on average) over a certain distance in the tissue, the mean value of $\sqrt{P}\frac{d\gamma}{dx}$ can be neglected, so that, in that region of the tissue, Eq. A8

gives

$$\bar{\gamma} \cong -\sqrt{\frac{Q}{2\alpha_R D_R}} \cong -\sqrt{\frac{\bar{Q}}{2\alpha_R D_R}}, \qquad \text{A9}$$

where the bars indicate that the relation holds only for mean values.

We have obtained with Eq. A9 a generalization of A5. In the same way, it is possible to show that the relation A6 is still valid (to a first approximation) with Q replaced by $\bar{Q}$, provided that γ remains relatively constant on average in the oxygenated layer of tissue.

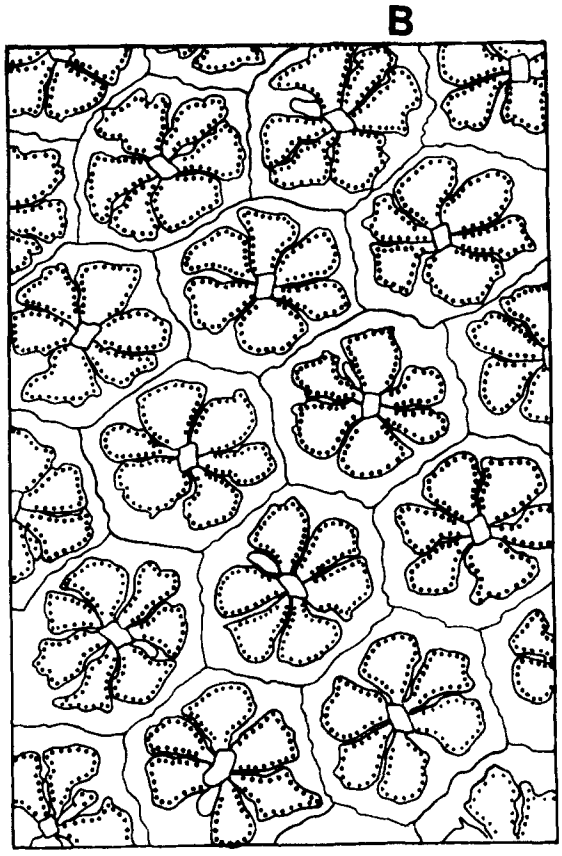

FIGURE 12.

To illustrate this result we have drawn the plots of $\sqrt{P(x)}$ and $\frac{P_o - P}{x}$ for two different cases, namely, when Q is constant and when it is periodical, $\bar{Q}$ being the same in both cases. The choice of a periodical form for Q seems reasonable, inasmuch as the drone retina is made up of ommatidia that form repeating units ~30 μm in diameter and because in the ommatidia most of the oxygen is expected to be consumed in the photoreceptors because of the presence of mitochondria (see Fig. 12 *B*). The values plotted in Fig. 12 *A* are those obtained when the length of one period of $Q(x)$

is chosen to be 31.4 μm, and they are nearly identical to those obtained from Eqs. A5 and A6. Therefore, we conclude that the histological structure of the retina does not substantially affect the validity of Eqs. A5 and A6.

To plot our results, we have chosen to use relation A5 rather than A6, mainly for two reasons: (*a*) it is more relevant to have the variables x and P plotted independently and (*b*) the error in measuring $\sqrt{P}$ in the well-oxygenated part of the tissue ($P_{O_2} > 50$ mm Hg; see Results) is relatively constant, so that the estimation of γ is straightforward.

Mr. J. L. Munoz provided expert technical assistance and Dr. J. A. Coles helped in preparing the manuscript. Mr. D. Pollet made the perfusion chamber. Miss Ch. Friedli pointed out in the early stages of this study the possibility of measuring the oxygen consumption with a microelectrode. We thank Drs. I. Fatt, A. Gardner-Medwin, A. Mauro, F. Baumann, and Th. Goldstick for helpful criticism of the manuscript.

This work was supported by Swiss National Scientific Foundation grant 3.339.078 and the Georges Kernen Foundation for Research on the Retina.

Received for publication 23 September 1980.

REFERENCES

ALTMAN, P. L., and D. S. DITTMER. 1971. Respiration and Circulation. Federation of American Societies for Experimental Biology, Bethesda. 17–18.

AUTRUM, H., and K. HAMDORF. 1964. Der Sauerstoffverbrauch des Bienenauges in Abhängigkeit von der Temperatur, bei Belichtung und im Dunkeln. *Z. Vgl. Physiol.* **48:**266–269.

AUTRUM, H., and T. TSCHARNTKE. 1962. Der Sauerstoffverbrauch der Insektenretina im Licht und Dunkeln. *Z. Vgl. Physiol.* **45:**695–710.

BATTINO, R., EVANS, F. D., and W. F. DANFORTH. 1968. The solubilities of seven gases in olive oil with reference to theories of transport through the cell membrane. *J. Am. Oil Chem. Soc.* **45:** 830–833.

BAUMANN, F. 1968. Slow and spike potentials recorded from retinula cells of the honeybee drone in response to light. *J. Gen. Physiol.* **52:**855–875.

BAUMANN, F. 1974. Electrophysiological properties of the honey bee retina. *In* The Compound Eye and Vision of Insects. C. A. Horridge, Editor. Clarendon Press, Oxford. 53–74.

BAUMANN, F., and A. MAURO. 1973. Effect of hypoxia on the change in membrane conductance evoked by illumination in arthropod photoreceptors. *Nat. New Biol.* **244:**146–148.

BURNEL, M., MAHLER, H. Q., and W. J. MOORE. 1970. Protein synthesis in visual cells of *Limulus* more important in dark than light. *J. Neurochem.* **17:**1493–1499.

BORSELLINO, A., and M. C. F. FUORTES. 1968. Interpretation of responses of visual cells of *Limulus*. *Proc. IEEE* **56:**1024–1032.

COLES, J. A., and M. TSACOPOULOS. 1979. Potassium activity in photoreceptors, glial cells and extracellular space in the drone retina: changes during photostimulation. *J. Physiol. (Lond.).* **290:**525–549.

CONNELLY, C. M., BRONK, D. W., and F. BRINK. 1953. A sensitive respirometer for the measurement of rapid changes in metabolism of oxygen. *Rev. Sci. Instrum.* **24:**683–695.

CRANK, J., and R. S. GUPTA. 1972. A moving boundary problem arising from the diffusion of oxygen in absorbing tissue. *J. Inst. Math. Its Appl.* **10:**19–33.

DAVIES, P. W. 1962. The oxygen cathode. *Phys. Tech. Biol. Res.* **4:**137–179.

EVANS, N. T. S., and T. B. CONSTABLE. 1976. A method for measuring oxygen uptake rate distributions over the surface zone of excised tissues using a 91-cathode electrode. *Adv. Exp. Med. Biol.* **75:**25–32.

EVANS, N. T. S., and A. R. GOURLAY. 1977. The solution of a two-dimensional time-dependent diffusion problem concerned with oxygen metabolism in tissues. *J. Inst. Math. Its Appl.* **19:** 239–251.

EVÊQUOZ, V., DESHUSSES, J., and M. TSACOPOULOS. 1978. The effect of photostimulation on glycogen turnover in the retina of the honeybee drone. *Experientia.* **34:**897. (Abstr.).

FATT, D. 1976. Polarographic Oxygen Sensor. CRC Press, Inc., Cleveland.

GANFIELD, R. A., NAIR, P., and W. J. WHALEN. 1970. Mass transfer, storage, and utilization of O_2 in cat cerebral cortex. *Am. J. Physiol.* **219:**814–821.

GOLDSTICK, T. K., and I. FATT. 1970. Diffusion of oxygen in solutions of blood proteins. *Chem. Eng. Prog. Symp. Ser.* **66:**101–113.

GORE, R. W., and W. J. WHALEN. 1968. Relations among tissue PO_2, QO_2 and resting heat production of frog sartorius muscle. *Am. J. Physiol.* **214:**277–286.

HAMDORF, K., and A. H. KASCHEF. 1964. Der Sauerstoffverbrauch des Facettenauges von *Calliphora erythrocephala* in Abhängigkeit von der Temperatur und dem Ionenmilieu. *Z. Vgl. Physiol.* **48:**251–265.

HARRIS, S. I., BALABAN, R. S., and L. J. MANDEL. 1980. Oxygen consumption and cellular ion transport: evidence for adenosine triphosphate to O_2 ratio near 6 in intact cell. *Science (Wash. D. C.).* **208:**1148–1150.

HILL, A. V. 1928. The diffusion of oxygen and lactic acid through tissues. *Proc. R. Soc. Lond. B Biol. Sci.* **104:**39–96.

HILL, D. K. 1948. Oxygen tension and the respiration of resting frog's muscle. *J. Physiol. (Lond.).* **107:**479–495.

LANTZ, C., and A. MAURO. 1978. Alteration of sensitivity and time scale in invertebrate photoreceptors exposed to anoxia, dinitrophenol, and carbon dioxide. *J. Gen. Physiol.* **72:**219–231.

LEHMENKÜHLER, A., H. CASPERS, and E. J. SPECKMANN. 1976. A method for simultaneous measurements of bioelectric activity and local tissue PO_2 in the CNS. *Adv. Exp. Med. Biol.* **75:** 3–7.

LEVICH, V. 1962. Physico-chemical Hydrodynamics. Prentice-Hall, Inc., Englewood Cliffs.

MAHLER, M. 1978 *a*. Diffusion and consumption of oxygen in the resting frog sartorius muscle. *J. Gen. Physiol.* **71:**533–557.

MAHLER, M., 1978 *b*. Kinetics of oxygen consumption after a single isometric tetanus of the frog sartorius muscle at 20°C. *J. Gen. Physiol.* **71:**559–593.

MAHLER, M. 1981. Diffusion in an elliptical cylinder. A reassessment of the diffusion coefficient for oxygen in muscle. *Biophys. J.* **33** (2, Pt. 2):25 *a* (Abstr.).

PEPE, M., and F. BAUMANN. 1972. Incorporation of ^{3}H-labelled leucine into a protein fraction in the retina of the honeybee drone. *J. Neurochem.* **19:**507–512.

PERRELET, A. 1970. The fine structure of the retina of the honeybee drone. *Z. Zellforsch. Mikrosk. Anat.* **108:**530–562.

PERRELET, A. 1972. Protein synthesis in the visual cells of the honey bee drone as studied with electron microscope radioautography. *J. Cell Biol.* **55:**595–605.

RANG, H. P., and J. M. RITCHIE. 1968. The dependence on external cations of the oxygen consumption of mammalian non-myelinated fibres at rest and during activity. *J. Physiol. (Lond.).* **196:**163–181.

SCHNEIDERMAN, G. 1975. A theoretical study of oxygen microelectrode design criteria and performance characteristics. Ph.D. Dissertation, Northwestern University, Evanston, Illinois.

SCHNEIDERMAN, G., and T. K. GOLDSTICK. 1976. Oxygen fields induced by recessed and needle oxygen microelectrodes in homogeneous media. *Adv. Exp. Med. Biol.* **75:**9–16.

STEIN, P. J., J. D. BRAMMER, and S. E. OSTROY. 1979. Renewal of opsin in the photoreceptor cells of the mosquito. *J. Gen. Physiol.* **74:**565–582.

TAKAHASHI, G. H., I. FATT, and T. K. GOLDSTICK. 1966. Oxygen consumption rate of tissue measured by a micropolarographic method. *J. Gen. Physiol.* **50:**317–335.

TSACOPOULOS, M., and A. LEHMENKÜHLER. 1977. A double-barrelled Pt microelectrode for simultaneous measurement of PO_2 and bioelectrical activity in excitable tissues. *Experientia.* **33:**1337–1338.

WANG, J. 1954. Theory of the self-diffusion of water in protein solutions. A new method of studying the hydration and shape of protein molecules. *J. Am. Chem. Soc.* **76:**4755–4763.

WHALEN, W. J., J. RILEY, and P. NAIR. 1967. A microelectrode for measuring intracellular PO_2. *J. Appl. Physiol.* **23:**798–801.

WIERNSBERGER, N., S. KUNKE, and P. GIGAX. 1976. Technical note about simultaneous recording of O_2 partial pressure and neuronal activity in cat cortex. *Experientia.* **32:**671–673.

WIGGLESWORTH, V. B. 1931. The respiration of insects. *Biol. Rev. Camb. Philos. Soc.* **6:**181–220.

WONG, F., C. F. WU, A. MAURO, and W. P. PAK. 1976. Persistence of prolonged light-induced conductance change in arthropod photoreceptors on recovery from anoxia. *Nature (Lond.).* **264:**661–664.

WYMAN, J. 1966. Facilitated diffusion and the possible role of myoglobin as a transport mechanism. *J. Biol. Chem.* **241:**115–121.

ZANDER, R. 1976. Cellular oxygen concentration. *Adv. Exp. Med. Biol.* **75:**463–467.